

2-Oxo-histidine-containing dipeptides are functional oxidation products

Hideshi Ihara<sup>1</sup>\* #, Yuki Kakihana<sup>1</sup> #, Akane Yamakage<sup>1</sup>, Kenji Kai<sup>2</sup>, Takahiro Shibata<sup>3</sup>,  
Motohiro Nishida<sup>4</sup>, Ken-ichi Yamada<sup>5,6</sup>, and Koji Uchida<sup>3,6,7</sup>\*

From the <sup>1</sup>Department of Biological Science, Graduate School of Science, Osaka Prefecture University, Sakai, Osaka 599-8531, Japan; <sup>2</sup>Department of Biological Chemistry, Graduate School of Life and Environmental Sciences, Osaka Prefecture University, Sakai, Osaka 599-8531, Japan; <sup>3</sup>Graduate School of Bioagricultural Sciences, Nagoya University, Nagoya 464-8601, Japan; <sup>4</sup>Division of Cardiocirculatory Signaling, National Institute for Physiological Sciences, Okazaki 444-8787, Japan; <sup>5</sup>Physical Chemistry for Life Science Laboratory, Faculty of Pharmaceutical Sciences, Kyushu University, Fukuoka, Japan; <sup>6</sup>Japan Agency for Medical Research and Development, CREST, Tokyo, Japan; <sup>7</sup>Graduate School of Agricultural and Life Sciences, The University of Tokyo, Tokyo 113-8657, Japan

Running title: *2-Oxo-IDPs are functional oxidation products*

# These authors contributed equally to this work.

\* To whom correspondence should be addressed:

Hideshi Ihara: Department of Biological Science, Graduate School of Science, Osaka Prefecture University, Sakai, Osaka 599-8531, Japan: [ihara@b.s.osakafu-u.ac.jp](mailto:ihara@b.s.osakafu-u.ac.jp); Tel.81-72-254-9753; Fax. 81-72-254-9163

Koji Uchida: Graduate School of Agricultural and Life Sciences, The University of Tokyo, Tokyo 113-8657, Japan: [a-uchida@mail.ecc.u-tokyo.ac.jp](mailto:a-uchida@mail.ecc.u-tokyo.ac.jp); Tel.81-3-5841-5127; Fax. 81-3-5841-8026

**Keywords:** 2-oxo-histidine-containing dipeptides, carnosine, anserine, homocarnosine, antioxidant activity, neuroprotection, oxidative stress, imidazole, histidine

---

## ABSTRACT

Imidazole-containing dipeptides (IDPs), such as carnosine and anserine, are found exclusively in various animal tissues, especially in the skeletal muscles and nerves. IDPs have antioxidant activity owing to their metal-chelating and free radical-scavenging properties. However, the underlying mechanisms that would fully explain IDPs' antioxidant effects remain obscure. Here, using HPLC–electrospray ionization–tandem MS analyses, we comprehensively investigated carnosine and its related small peptides in the soluble fractions of mouse tissue homogenates and ubiquitously detected 2-oxo-histidine-containing dipeptides

(2-oxo-IDPs) in all examined tissues. We noted enhanced production of the 2-oxo-IDPs in the brain of a mouse model of sepsis-associated encephalopathy. Moreover, in SH-SY5Y human neuroblastoma cells stably expressing carnosine synthase, H<sub>2</sub>O<sub>2</sub> exposure resulted in the intracellular production of 2-oxo-carnosine, which was associated with significant inhibition of the H<sub>2</sub>O<sub>2</sub> cytotoxicity. Notably, 2-oxo-carnosine showed a better antioxidant activity than endogenous antioxidants such as glutathione and ascorbate. Mechanistic studies indicated that carnosine monooxygenation is mediated through the formation of a histidyl-imidazole radical, followed by the addition of

molecular oxygen. Our findings reveal that 2-oxo-IDPs are metal-catalyzed oxidation products present *in vivo* and provide a revised paradigm for understanding the antioxidant effects of the IDPs.

---

The mammalian essential amino acid, L-histidine, and its methylated derivatives (1- and 3-methylhistidines) are known to be widely and abundantly distributed in mammalian tissues in their free form or as components of peptides and proteins. Carnosine ( $\beta$ -alanyl-L-histidine), which was first discovered over 100 years ago, is the most well characterized imidazole-containing dipeptide (IDP). Since then, carnosine and other IDPs, such as anserine ( $\beta$ -alanyl-3-methyl-L-histidine) and homocarnosine ( $\gamma$ -aminobutyryl-L-histidine), have been observed at high concentrations in the skeletal muscles and central nervous systems of many vertebrates (1). The levels of the IDPs are regulated by metabolic enzymes, including carnosine synthase (CARNS) (2), methyltransferase (3), and dipeptidase (4,5), indicating that IDPs play physiological roles in the muscle and brain. It has been postulated that carnosine contributes significantly to physicochemical buffering in skeletal muscles by neutralizing the lactic acid produced during anaerobic glycolysis (6). Evidence has also been found that the peptide may play a role as a neurotransmitter in olfactory receptor axons (7) and as a regulator of enzymes (8). In addition to these functions, carnosine has attracted a lot of attention as a potential antioxidant due to its reactivity with reactive oxygen and nitrogen species, and its potential to form adducts with deleterious aldehydes and ketones (1). Carnosine also shows an efficient metal-chelating property, which may be associated with its antioxidant activity (1). However, the exact antioxidant mechanisms of the peptide remain unknown.

Due to the metal-chelating property of the imidazole ring, histidine is extremely sensitive to metal-catalyzed oxidation reactions. In the presence of oxygen and a reducing agent, such as ascorbate, the binding of metal ions, such as copper ion ( $\text{Cu}^{2+}$ ), to histidine results in the facile oxidation of its imidazole ring. The reaction involves the reduction of  $\text{Cu}^{2+}$  by the reducing agent to generate  $\text{Cu}^+$ . The reduced form of copper ion donates one electron to  $\text{O}_2$  to generate an unidentified reactive oxygen species, which immediately oxidizes the ligand itself (histidine). It has been reported that the metal-catalyzed oxidation of histidine generates a number of products, including a unique monooxygenation product, 2-oxo-histidine. (9-11) The formation of 2-oxo-histidine has been demonstrated in the peptides and proteins *in vitro* and implicated in aging and other pathological states associated with oxidative stress (9-11). However, no study has definitively demonstrated the presence of 2-oxo-histidine *in vivo*.

In the present study, we unambiguously detected 2-oxo-histidine-containing dipeptides (2-oxo-IDPs) in mouse tissue homogenates using high performance liquid chromatography with online electrospray ionization tandem mass spectrometry (LC-ESI-MS/MS). To the best of our knowledge, this is the first evidence for the presence of oxidized peptides containing 2-oxo-histidine *in vivo*. In addition, using human neuroblastoma cells stably expressing CARNS, we demonstrated significant inhibition of the  $\text{H}_2\text{O}_2$  cytotoxicity and a concomitant increase in the intracellular levels of the 2-oxo-IDPs. We also found that IDPs gain a free radical scavenging activity via the oxygenation. Mechanistic studies of the metal-catalyzed oxidation of IDPs demonstrate that the monooxygenation of IDPs may be mediated through the formation of a histidyl radical followed by the addition of molecular oxygen. These results reveal new insights into the antioxidant function of the IDPs.

## Results

### *Comprehensive analysis of IDPs in mouse muscle homogenates*

To simultaneously detect carnosine and related peptides *in vivo*, we sought to identify a common fragment ion from the MS/MS product-ion analysis of the authentic peptides. The product-ion analysis of carnosine gave common fragments at the mass-to-charge ratios ( $m/z$ ) of 89 and 72, corresponding to the cleavage at the peptide bond, and at the N-C $\alpha$  bond in the peptide backbone, respectively (**Fig. S1**). Similarly, anserine gave the same fragment ions (**Fig. S2**). These characteristic common fragment ions allowed the simultaneous analysis of carnosine and anserine using LC-ESI-MS/MS in the multiple reaction monitoring (**Fig. S3**). We then applied this method to the tissue samples to detect the IDPs. As shown in **Fig. 1A**, the IDPs were detected in mouse muscle along with several unknown peptides. Identifications were tentatively made by comparison of the retention time and mass-to-charge ratio, indicating that the peptides **1** ( $m/z$  227) and **2** ( $m/z$  241) were identical to carnosine and anserine, respectively. We also detected six other peptides: two (peptides **3** and **4**) of them showed molecular ions at  $m/z$  243 and 257 ( $[M+H]^+$ ), corresponding to a 16-Da increase in the mass value of carnosine and anserine, respectively. It was speculated that, because this change in molecular weight could originate from the mono-oxygenation of the imidazole groups, the products might contain an oxo-imidazole moiety.

### *Identification of oxidized IDPs*

The formation of 2-oxo-histidine is now known to be due to the metal-catalyzed oxidation of histidine (12). Hence, to confirm the structure of the products, carnosine and anserine were incubated with ascorbate in the presence of Cu<sup>2+</sup>, and the reaction mixtures were analyzed by LC-ESI-MS/MS. The data

(**Fig. S4**) showed that products **3** and **4** were indistinguishable from  $\beta$ -alanyl-L-2-oxo-histidine (2-oxo-carnosine) and  $\beta$ -alanyl-3-methyl-L-2-oxo-histidine (2-oxo-anserine), respectively (**Fig. 1B**).

Despite its abundance in the *in vitro* oxidized proteins, the presence of 2-oxo-histidine *in vivo* has never been demonstrated. To accurately analyze the endogenous formation of 2-oxo-IDPs in cells and tissues, we established a highly sensitive and specific method for the measurement of 2-oxo-IDPs using LC-ESI-MS/MS coupled with a stable isotope dilution method. Collision-induced dissociation of purified 2-oxo-carnosine showed relevant products at  $m/z$  89.0 and  $m/z$  196.1 (**Fig. S5A**). The product ions at  $m/z$  89.0 and  $m/z$  196.1 matched values expected to originate from a  $\beta$ -alanine moiety and 2-oxo-carnosine, respectively. The identification of these product ions was supported by the observation that the collision-induced dissociation of the standard isotope-labeled 2-oxo-carnosine, containing [<sup>13</sup>C<sub>3</sub>,<sup>15</sup>N]  $\beta$ -alanine, produced relevant product ions at  $m/z$  93.0 and  $m/z$  198.1 (**Fig. S5B**). **Fig. S5C** demonstrates the result on the standard isotope-labeled carnosine and non-labeled carnosine using multiple reaction monitoring (MRM) between the transition from the protonated parent ions  $[M + H]^+$  to the characteristic daughter ions,  $m/z$  247.1 $\rightarrow$ 198.1 and  $m/z$  243.1 $\rightarrow$ 196.1. This allowed detection of both the standard isotope-labeled and non-labeled carnosine, respectively. The characterization of 2-oxo-anserine and 2-oxo-homocarnosine was also performed in a similar way to 2-oxo-carnosine (data not shown). Parameters for the MRM analysis of the IDPs and 2-oxo-IDPs are summarized in **Table S1**. The LOQ (limit of quantification) for the 2-oxo-IDPs was 100 fmol on the column with linearity ( $r^2 = 0.999$  (100–5000 fmol)).

Using the LC-ESI-MS/MS coupled with a stable isotope dilution method, we analyzed the IDPs and 2-oxo-IDPs in several mouse

tissues. Endogenous carnosine and 2-oxo-carnosine were co-eluted with the spiked standards labeled with the stable isotope at the same retention time (**Figs. 2A, B**). Results of the quantitative identification of the IDPs and their 2-oxo products are summarized in **Fig. 2C**. The data showed that the levels of 2-oxo-carnosine were 0.23, 2.1, and 4.8 pmol/mg protein in the brain, kidney, and muscle, respectively, while the corresponding levels of carnosine were 1968, 120, and 18921 pmol/mg protein, respectively. Carnosine was also detected in the lung, heart, and liver at 86, 224, and 11 pmol/mg protein, respectively. The percentages of 2-oxo-carnosine to carnosine were 0.012, 1.8, and 0.025% in the brain, kidney, and muscle, respectively. 2-Oxo-anserine was detected in all the tested tissues at 0.11, 0.45, 0.36, 7.0, 0.33, and 30 pmol/mg protein in brain, lung, heart, kidney, liver, and muscle, respectively, and the corresponding levels of anserine were 67, 116, 65, 211, 17, and 15990 pmol/mg protein, respectively. 2-Oxo-homocarnosine was detected only in the brain at 0.89 pmol/mg protein, consistent with the result that homocarnosine was mainly detected in the brain (570 pmol/mg protein).

#### ***Enhanced production of 2-oxo-IDPs in a mouse model of sepsis-associated encephalopathy (SAE)***

It has been reported that IDPs show an antioxidant activity through metal-chelating and free radical-scavenging mechanisms (1). Therefore, it was speculated that the presence of 2-oxo-IDPs *in vivo* might reflect the antioxidant activity of the IDPs. To assess the involvement of oxidative stress in the mono-oxygenation of histidine residues in the IDPs, we quantitatively analyzed the 2-oxo-IDPs in the brain of a mouse model of SAE, an acute brain dysfunction resulting from a systemic inflammatory response using LC-ESI-MS/MS coupled with stable isotope dilution methods. After lipopolysaccharide (LPS) injection, symptoms

of sepsis, including exhaustion and body-weight loss, were observed (**Fig. 3A**). The levels of the 2-thiobarbituric acid reactive substances (TBARS), a marker of oxidative stress, in the brain significantly increased 24 h after the injection of LPS (**Fig. 3B**), suggesting that oxidative stress was enhanced in the brains of the SAE mouse. The brain levels of the IDPs (carnosine, anserine, and homocarnosine) were nearly unchanged under these conditions (data not shown). However, the levels of 2-oxo-carnosine were transiently elevated 8 h after injection and returned to the control levels after 24 h (**Figs. 3C, D**). A similar pattern was also observed for the other 2-oxo-IDPs, including 2-oxo-anserine (**Fig. 3E**) and 2-oxo-homocarnosine (**Fig. 3F**). The transient increases in 2-oxo-IDPs may relate to their turnover rates *in vivo* and may be associated with the low levels of 2-oxo-IDPs in tissues (**Fig. 2**). These data are in line with the fact that oxidative stress occurs in the early stages of sepsis (13).

#### ***Enhanced production of 2-oxo-carnosine in CARNS-overexpressed cells exposed to oxidants***

To further assess the relationship between the production of the 2-oxo-IDPs and oxidative stress, we generated SH-SY5Y cells stably expressing CARNS (**Fig. 4A**) and examined the production of 2-oxo-carnosine following exposure of the cells to H<sub>2</sub>O<sub>2</sub>. In the presence of H<sub>2</sub>O<sub>2</sub>, the cell lysates of the SH-SY5Y cells expressing CARNS showed that the levels of carnosine were approximately 20 nmol/mg protein, which was 240-fold higher than in the control cell lysates (**Fig. 4B**). We then examined the effect of the CARNS overexpression on the cytotoxicity caused by H<sub>2</sub>O<sub>2</sub>. H<sub>2</sub>O<sub>2</sub> showed a toxicity to both the control and CARNS-expressing cells; however, the cells overexpressing CARNS were more resistant to the H<sub>2</sub>O<sub>2</sub> cytotoxicity than the control cells (**Fig. 4C**). In addition, concomitant

to the reduction of the H<sub>2</sub>O<sub>2</sub> cytotoxicity, an enhanced production of 2-oxo-carnosine was observed (**Fig. 4D**). To assess the involvement of the intracellular H<sub>2</sub>O<sub>2</sub> in the enhanced production of 2-oxo-carnosine, we examined the effect of the membrane-permeable PEG-catalase. We observed that the production of 2-oxo-carnosine was completely inhibited by pretreatment with the antioxidant enzyme (**Fig. 4E**). A similar cytoprotective effect of the CARNS overexpression was observed in the rotenone-induced cytotoxicity (**Figs. 4F–H**). These data suggest that the production of the 2-oxo derivatives may reflect the antioxidant activity of the IDPs.

### ***Gain of antioxidant function***

To establish that the monooxygenation is involved in the gain of antioxidant function of the IDPs, we examined the free radical scavenging activity of carnosine and its oxidized product (2-oxo-carnosine) using the Trolox equivalent antioxidant capacity (TEAC) assay. Carnosine showed a negligible antioxidant activity (TEAC value = 0.0088 μmol/mmol). Strikingly, however, the TEAC of 2-oxo-carnosine was far greater (35,000-fold) than that of carnosine (**Fig. 5A**). In addition, the oxidized carnosine showed a better free radical scavenging activity than the endogenous antioxidants, such as glutathione and ascorbate. Incubation with the stable radical, 1,1-diphenyl-2-picrylhydrazyl (DPPH) resulted in the loss of 2-oxo-carnosine (**Fig. 5B**), which was accompanied by the formation of a product with a molecular ion at  $m/z$  of 620 ( $[M+H]^+$ ) (data not shown). This change in the molecular weight corresponds to a 393-Da increase, accounting for the molecular mass of DPPH, in the mass value of the unmodified carnosine. The detailed mechanism of how 2-oxo-carnosine forms the product with DPPH remains unknown. We also assessed the cytoprotective effect of 2-oxo-carnosine on the rotenone-induced neuronal cell death. In our

preliminary experiments, we examined the cytoprotective effect of 2-oxo-carnosine at concentrations ranging from 0 to 400 μM and observed that 2-oxo-carnosine concentrations of as low as 50 μM showed significant effect (data not shown). As shown in **Fig. 5C**, the oxidized carnosine was slightly more effective than its unoxidized form.

### ***A mechanism for the conversion of IDPs to 2-oxo-IDPs***

To gain an insight into the formation of the 2-oxo-IDPs *in vivo*, we characterized the mechanism for the conversion of IDPs to the 2-oxo-IDPs by Cu<sup>2+</sup>/ascorbate *in vitro*. As shown in **Fig. 6A**, both Cu<sup>2+</sup> and ascorbate were essential for the formation of 2-oxo-carnosine. Similar patterns were observed for anserine and homocarnosine (**Fig. S6**). To identify the origin of oxygen in the 2-oxo-imidazole ring, we examined the incorporation of <sup>18</sup>O from <sup>18</sup>O<sub>2</sub> and H<sub>2</sub><sup>18</sup>O in carnosine. As shown in **Fig. 6B**, 2-[<sup>18</sup>O] oxo-carnosine was detected in the reaction mixture containing <sup>18</sup>O<sub>2</sub>, but not H<sub>2</sub><sup>18</sup>O, indicating that oxygen at the C2 position of 2-oxo-carnosine is derived from molecular oxygen. This result strongly suggests the formation of an imidazole radical as the intermediate.

To detect the imidazole radical intermediate, a spin-trapping reagent, 4-amino-2,2,6,6-tetramethylpiperidiny-1-oxy (amino-TEMPO•), which converts radicals into stable diamagnetic adducts, was used for the mass spectrometry-based detection of biologically relevant carbon-centered free radicals. When carnosine was incubated with Cu<sup>2+</sup>/ascorbate in the presence of amino-TEMPO•, a putative amino TEMPO-carnosine adduct was detected at  $m/z$  399 (**Figs. 7A, B**). Collision-induced dissociation of the adduct produced relevant product ions at  $m/z$  156.0 and 173.1 (**Fig. 7C**), which were consistent with a histidine moiety and an amino TEMPO moiety, respectively. The formation of the amino-TEMPO-carnosine

adduct was accompanied by the reduced formation of 2-oxo-carnosine (**Figs. 7D, E**), suggesting that the formation of imidazole radicals in the IDPs might be an intermediate step for the production of the 2-oxo derivatives. These data also support our hypothesis that the mono-oxygenation of the IDPs may be mediated through the formation of an imidazole radical followed by the addition of molecular oxygen (**Fig. 7F**).

## Discussion

A growing body of evidence shows the protective role of IDPs in ischemia/reperfusion damage and in human diseases such as diabetes, cataract, and neurodegenerative disorders (1). However, the underlying molecular mechanism for their beneficial effects remains unclear. In the present study, we adopted a mass spectrometry-based approach to analyze the IDPs in tissue samples. Taking advantage of the fact that the authentic IDPs we studied, including carnosine and anserine, commonly gave specific fragment ions at  $m/z$  72 and 89, we comprehensively analyzed the IDPs in mouse muscle homogenates and detected two unknown peptides, showing molecular ions at  $m/z$  243 and 257 ( $[M+H]^+$ ), corresponding to a 16-Da increase in the mass value of carnosine and anserine, respectively. Based on the LC-ESI-MS/MS analysis of the synthetic compounds, these derivatives were identical to 2-oxo-carnosine and 2-oxo-anserine. Thus, the comprehensive analysis of tissue IDPs unexpectedly led to the discovery of 2-oxo-IDPs *in vivo*. To the best of our knowledge, this is the first report demonstrating that the conversion of histidine to 2-oxo-histidine is a naturally-occurring reaction *in vivo*.

Our study on the quantification of IDPs using LC-ESI-MS/MS coupled with a stable isotope dilution method showed that, consistent with previous findings (1), both carnosine and anserine were mainly detected in skeletal muscle tissues. They were also measurable in

brain regions and other tissues as well, but at concentrations 10- to 1,000-fold lower than in muscle. We also quantified 2-oxo-IDPs in the tissue samples by LC-ESI-MS/MS. This method showed LOQs of approximately 100 fmol for the oxidized IDPs. The amount of 2-oxo-carnosine was 4.8 pmol/mg protein in the muscle tissue, which was several-fold higher than in other tissues. This was not surprising in view of the fact that carnosine is the most abundant dipeptide in the skeletal muscle. Similar to 2-oxo-carnosine, 2-oxo-anserine was mainly detected in the muscle tissue. However, the level of 2-oxo-anserine in the muscle tissue was 30 pmol/mg protein, which was significantly higher than that of 2-oxo-carnosine. This may be explained by the fact that the 1-methylimidazole derivatives are much more sensitive to mono-oxygenation than the imidazoles (14). 2-Oxo-homocarnosine was detected only in the brain samples at 0.89 pmol/mg protein. Thus, the quantities of the oxidized IDPs were shown to correlate with those of the original peptides in their respective tissues.

IDPs are believed to function as an antioxidant in muscle and brain. Several studies have indeed claimed that IDPs might exert their cytoprotective effect through their antioxidant activities in neuronal cells (15,16). However, no direct evidence that can satisfactorily explain this function has been reported. In the present study, we generated SH-SY5Y cells stably expressing CARNS and tested the effect of carnosine overproduction on neuronal cell death induced by oxidative stress. The CARNS-overexpressed SH-SY5Y neuroblastoma cells, showing high levels of intracellular carnosine, were resistant to cytotoxicity induced by H<sub>2</sub>O<sub>2</sub> and rotenone. More interestingly, following its antioxidant activity, the level of 2-oxo-carnosine was significantly elevated in cells treated with pro-oxidants. Along with the finding that membrane-permeable PEG-catalase inhibited the production of 2-oxo-

carnosine, these results support a generally accepted hypothesis that carnosine endogenously produced in cells functions as an antioxidant.

The discovery of 2-oxo-histidine was first reported by Uchida and Kawakishi in 1986 in their attempt to identify oxidized products generated during the metal-catalyzed oxidation ( $O_2/Cu^{2+}/ascorbate$ ) of histidine (12). They have also shown that 2-oxo-histidine further underwent oxidative degradation to generate ring-opened products such as aspartate, aspartylurea, and formylasparagine (17). Using HPLC with electrochemical detection, the formation of 2-oxo-histidine in oxidized proteins has been established *in vitro* (18). So far, 2-oxo-histidine has been detected in the *in vitro* oxidation of proteins, such as Cu/Zn-superoxide dismutase (19,20), human relaxin (21), vanadium bromoperoxidase (22), human growth hormone (23), oxidized low density lipoprotein (24), and prion protein (25). More recently, Traore et al. (26) provided evidence for the formation of 2-oxo-histidine during the oxidative inactivation of PerR, a metal-dependent sensor of  $H_2O_2$ . It has been proposed that the bound iron coordinates  $H_2O_2$  and generates a reactive species, which then directly reacts with the nearby histidine (27). The formation of 2-oxo-histidine has been suggested to be an  $H_2O_2$ -sensing mechanism by which PerR uses metal-catalyzed oxidation reactions to regulate the expression of oxidative defense genes. Given the fact that IDPs are efficient metal-chelating agents, the intracellular formation of 2-oxo-IDPs may be the result of metal-catalyzed oxidation reactions involving loosely-chelated metal ions. Thus, it is reasonable to speculate that the IDPs show their antioxidant activity when they bind metal ions to form IDP-metal complexes.

It has been shown that the antioxidant activity of IDPs is mediated by different mechanisms involving metal ion chelation and scavenging reactive oxygen species. However,

despite the numerous findings and mechanistic insights that revealed the antioxidant functions of IDPs, the exact antioxidant mechanism remained unknown. In the current studies, we characterized the free radical scavenging activity of 2-oxo-carnosine using the TEAC assay and unexpectedly discovered that the oxidized IDP scavenged the free radicals far more efficiently than its original form (**Fig. 5**). More strikingly, 2-oxo-carnosine showed a better antioxidant activity than glutathione and ascorbate, the two main aqueous-phase antioxidants within cells. Thus, the conversion of IDPs into their 2-oxo forms may, at least in part, explain their antioxidant activity. In addition, it can be speculated that the 2-oxo-IDPs may be converted to further oxidized products when they exert their free radical scavenging activity. We indeed detected the product with the molecular mass, corresponding to a DPPH-carnosine complex. However, the detailed mechanisms for the formation of the complex remain unknown. Certainly, further studies are needed to unravel mechanistic details concerning the antioxidant activity of the 2-oxo-IDPs.

The isolation and structural identification of 2-oxo-IDPs and their reaction intermediates in conjunction with isotopic incorporation studies have enabled us to propose a mechanism for the formation of 2-oxo-histidine (**Figs. 6 and 7**). Based on the result that the incorporation of  $^{18}O$  was only observed in the reaction mixture containing  $^{18}O_2$ , the oxygen atom introduced into the 2-oxo-IDPs might originate from  $O_2$  (**Fig. 6**). The initiating step may be H-abstraction from C-2 of the imidazole ring of histidine residues followed by the addition of  $O_2$  to form a peroxy radical. The 2-hydroperoxy-histidine has indeed been detected in  $H_2O_2$ -oxidized Cu/Zn-superoxide dismutase using a tandem quadrupole/orthogonal-acceleration time-of-flight (ESI-Q-TOF) mass spectrometer combined with a nano-HPLC system (19). A reactive species involving H-

abstraction from C-2 of the imidazole ring of histidine residues remains unclear; however, a high valent oxocopper species ( $\text{Cu}^{3+}=\text{O}$ ), a possible hydroxylating species, has previously been suggested as an intermediate in copper oxygenases, including tyrosinase and dopamine *p*-hydroxylase (28). The formation of 2-oxo-IDPs may therefore be mediated by the formation of  $\text{O}_2$ -metal-IDPs. These complexes could be associated with the formation of reactive species, such as  $\text{Cu}^{3+}=\text{O}$ , upon reaction with ascorbate followed by site-specific oxygenation of the imidazole ring in histidine residues. On the other hand, spin-trapping reagents have been shown to be highly effective probes for mass spectrometry-based detection of biologically-relevant carbon-centered free radicals. Hence, to gain insight into the formation of imidazole-based free radicals, we tested amino-TEMPO• as a spin-trapping reagent and successfully detected an amino-TEMPO-carnosine adduct by LC-ESI-MS/MS (Fig. 7). These data provide the first mechanistic details of the mono-oxygenation of IDPs, in which the metal-catalyzed oxidation reaction is mediated through the formation of an imidazole radical intermediate, followed by the addition of molecular oxygen.

In summary, we analyzed IDPs in mouse tissue homogenates and unambiguously detected 2-oxo-IDPs. In addition, we showed that the overexpression of CARN5 resulted in a significant inhibition of the  $\text{H}_2\text{O}_2$  cytotoxicity and a concomitant increase in the intracellular levels of the 2-oxo-IDPs. Notably, 2-oxo-carnosine showed better antioxidant activity than endogenous antioxidants, such as glutathione and ascorbate. Mechanistic studies of the metal-catalyzed oxidation of IDPs revealed that the mono-oxygenation of IDPs might be mediated through the formation of a histidyl radical intermediate, followed by the addition of molecular oxygen. The work described here is the first example of the *in vivo* detection of 2-oxo-histidine-containing

peptides formed during the oxygenation of natural IDPs of high medicinal interest. We thus provide a novel paradigm to understand the antioxidant effects of IDPs. One could also speculate that IDPs showing a beneficial antioxidant effect may gain a new function after converting to 2-oxo derivatives. Studies into this possibility represent an attractive future area of investigation.

## Experimental procedures

### Materials

L-Histidine,  $\beta$ -alanine,  $\gamma$ -aminobutyric acid, *p*-toluenesulfonic acid (TsOH), thionyl chloride, and *N,N*-dimethylacetamide were purchased from Nacalai Tesque (Kyoto, Japan). 3-Methyl-L-histidine, [ $^{13}\text{C}_3$ ,  $^{15}\text{N}$ ]  $\beta$ -alanine, and LPS (from *Escherichia coli*; O26:B6) were from Sigma-Aldrich (St Louis, MO, USA). [ $^{15}\text{N}_3$ ] L-histidine, [ $^{18}\text{O}$ ]  $\text{O}_2$ , and [ $^{18}\text{O}$ ]  $\text{H}_2\text{O}$  were obtained from the Taiyo Nippon Sanso Corporation (Tokyo, Japan). PEGylated catalase (PEG-catalase) was prepared as previously reported (29). Rotenone was purchased from Tokyo Chemical Industry Co., Ltd. (Tokyo, Japan). Toluene and Dulbecco's modified Eagle's medium (DMEM) were purchased from Wako Pure Chemical Industry (Osaka, Japan). Fetal bovine serum (FBS) was obtained from MultiSer (Cytosystems, Castle Hill, NSW, Australia). 3-(4,5-Dimethylthiazol-2-yl)-2,5-diphenyltetrazolium bromide (MTT) was from Dojindo Laboratories (Kumamoto, Japan). All other chemicals and reagents were from common suppliers and were of the highest commercially-available grade.

### Preparation of stable isotope-labeled IDPs

To prepare the isotope-labeled IDPs, 0.225 mmol of [ $^{13}\text{C}_3$ ,  $^{15}\text{N}$ ]  $\beta$ -alanine was treated with 0.45 mmol of TsOH in water (0.1 mL) for 30 min at room temperature, dried *in vacuo* and then dissolved in toluene (0.4 mL).  $\beta$ -Alanine•TsOH was dried *in vacuo* again. L-Histidine•2TsOH was prepared by the above-

mentioned method using 0.45 mmol of L-histidine and 0.90 mmol of TsOH.  $\beta$ -Alanine•TsOH was redissolved in thionyl chloride (0.6 mL) and incubated for 1 h at room temperature, dried *in vacuo* and then dissolved in toluene (0.4 mL).  $\beta$ -alanineCl•TsOH was dried *in vacuo* again. All the synthesized  $\beta$ -alanineCl•TsOH and L-histidine•2TsOH were mixed in *N,N*-dimethylacetamide (0.45 mL), purged with nitrogen, and incubated for 1 h at 4 °C with shaking. An equal amount of water was added to the mixture to hydrolyze the unreacted  $\beta$ -alanineCl•TsOH. The obtained [ $^{13}\text{C}_3$ ,  $^{15}\text{N}$ ] carnosine was purified by HPLC (JASCO Corporation, Tokyo, Japan) under the following conditions: a Scherzo SS-C18 column (6.0 x 100 mm, Imtakt, Kyoto, Japan) using a linear gradient of solvent A (water containing 0.1% formic acid) and solvent B (water containing 50% acetonitrile and 100 mM ammonium formate) (0% B at 0 min; 75% B at 20 min) at the flow rate of 1.0 mL/min. The elution was monitored by absorbance at 220 nm. 3-Methyl-L-histidine was used for the preparation of [ $^{13}\text{C}_3$ ,  $^{15}\text{N}$ ] anserine, instead of L-histidine.  $\gamma$ -Aminobutyric acid and [ $^{15}\text{N}_3$ ] L-histidine were used for the preparation of [ $^{15}\text{N}_3$ ] homocarnosine, instead of  $\beta$ -alanine and L-histidine, respectively. The chemical structures of the products were characterized by LC-ESI-MS/MS and NMR analyses.

#### Preparation of oxidized IDPs

Oxidation of the imidazole ring of the IDPs was carried out by the ascorbic acid-copper ion system (12). The reaction mixtures (5 mL) containing 10 mM IDPs, 200 mM sodium phosphate buffer (pH 7.2), 200 mM ascorbate, and 2 mM  $\text{CuSO}_4$  were incubated at room temperature. Oxygen gas was bubbled into the mixture for 30 min. The oxidized IDPs were purified under the following conditions: a Scherzo SS-C18 column (6.0 x 100 mm) using a linear gradient of solvent A (water containing 0.1% formic acid) and solvent B (water

containing 50% acetonitrile and 100 mM ammonium formate) (0% B at 0 min; 90% B at 20 min) at the flow rate of 1.5 mL/min. The elution was monitored by absorbance at 250 nm. The chemical structures of the products were characterized by LC-ESI-MS/MS and NMR analysis. The NMR analyses were performed using a JEOL JNM-ECZ500R (500 MHz) instrument. 2-Oxo-carnosine:  $^1\text{H}$  NMR ( $\text{D}_2\text{O}$ ):  $\delta\text{H}$  2.54 (dt,  $J = 3.5$  Hz, 2H), 2.66 (dd,  $J = 8.2$  Hz, 1H), 2.80 (dd,  $J = 5.5$  Hz, 1H), 3.06 (t,  $J = 6.8$  Hz, 2H), 4.41 (dd,  $J = 4.7$  Hz, 1H), 6.12 (s, 1H);  $\delta\text{C}$  31.34, 35.83, 39.70, 56.61, 119.01, 132.18, 159.10, 176.06, 179.17. 2-Oxo-anserine:  $^1\text{H}$  NMR ( $\text{D}_2\text{O}$ ):  $\delta\text{H}$  2.26 (dt,  $J = 3.1$  Hz, 2H), 2.60 (dd,  $J = 10$  Hz, 1H), 2.70 (t,  $J = 6.5$  Hz, 2H), 2.84 (m, 1H), 3.05 (s, 3H), 4.26 (dd,  $J = 4.7$  Hz, 1H), 6.12 (s, 1H);  $\delta\text{C}$  29.10, 31.92, 37.67, 38.87, 55.07, 117.95, 129.67, 155.86, 175.47, 179.10. 2-Oxo-homocarnosine:  $^1\text{H}$  NMR ( $\text{D}_2\text{O}$ ):  $\delta\text{H}$  1.72-1.75 (m, 2H), 2.21 (dt,  $J = 3.5$  Hz, 2H), 2.53 (dd,  $J = 8.2$  Hz, 1H), 2.76-2.81 (m, 3H), 4.23 (dd,  $J = 4.7$  Hz, 1H), 6.08 (s, 1H);  $\delta\text{C}$  24.41, 29.46, 33.86, 40.21, 55.46, 116.34, 129.51, 164.25, 175.61, 178.91.

#### LC-ESI-MS/MS analysis

The LC-ESI-MS/MS analyses were carried out using the Xevo TQD triple quadrupole mass spectrometer (Waters, MA, USA). Chromatography was carried out by an Intrada Amino Acid column (2.0 x 50 mm, Imtakt) using an Alliance e2695 system (Waters, MA, USA). A discontinuous gradient of solvent A (acetonitrile containing 0.1% formic acid) and solvent B (water containing 100 mM ammonium formate) was used as follows: 0% B at 0 min, 60% B at 0.1 min, 70% B at 5 min, 99% B at 9 min, at the flow rate of 0.3 mL/min. The mass spectrometer operated in the positive mode under the following conditions: capillary voltage 1000 V and desolvation gas (nitrogen) 1000 L/h at 500 °C. The oxidized imidazole dipeptides were identified and quantified in the

multiple reaction monitor (MRM) mode. The MRM parameters are listed in Table S1.

### ***Animal studies***

This study was performed in accordance with the Guidelines for Animal Experimentation of Osaka Prefecture University, Japan. All animal experiments were approved by the Animal Ethical Committee of Osaka Prefecture University. Nine-week-old male C57BL/6J mice (Kiwa Laboratory Animals Co., Ltd.; Wakayama, Japan) were reared at  $24 \pm 1$  °C and with a 12 h light/12 h dark cycle with free access to water and a standard diet for 1 week. For quantitative analysis, the mice (n = 3) were sacrificed. Blood was collected and serum was prepared, flash frozen and stored at -80 °C until processed. The lung, liver, heart, kidney, brain, and leg muscle were harvested, flash frozen and stored at -80 °C until processed. For oxidative stress experiments, the mice were divided into four groups (n = 3) and were intraperitoneally injected with LPS (10 mg/Kg of body weight) or quantified by the multiple reaction monitor (MRM) mode vehicle control (PBS). After injection for 0, 4, 8, or 24 h, the animals were weighed and sacrificed. The brains were harvested, flash frozen, and stored at -80 °C until processed.

### ***Preparation of mouse tissue samples***

Mouse tissues were homogenized with 10 volumes (w/v) of 80% acetonitrile in water containing 50 pmol of stable isotope-labeled standards using a Heidolph homogenizer (Heidolph, BY, Germany). The homogenates were centrifuged at 18,800 g for 20 min at 4 °C. The supernatants were collected and concentrated by a vacuum concentrator until the acetonitrile was removed. After the samples were mixed with equal amounts of ethyl acetate, an aqueous layer was obtained. The aqueous layer was diluted 4-fold with 100 mM HCl and applied on an Oasis MCX cartridge (Waters)

equilibrated with 100 mM HCl. The cartridge was washed with 5 column volumes of methanol, then the sample was eluted with 3 column volumes of 0.5 M ammonia in methanol. The samples were then dried *in vacuo*, dissolved in 0.1 mL of 2% formic acid in water, and subjected to an LC-ESI-MS/MS.

### ***Preparation of SH-SY5Y stable cell line overexpressing CARNS***

The *CARNS* gene (NP\_00159694) was amplified from human brain cDNA using primers: forward, 5'-CACCATGCACCATCATCATCATTCTTCTGGTCTCTCCCTGGATCCATCGGGTCCG-3' and reverse, 5'-CTATTTGAAGTGAGACAGGAAGTGGGC-3'. The amplified *CARNS* gene was cloned into the pENTR/D-TOPO vector using the directional TOPO cloning system (Gateway Cloning Technology, Thermo Fischer Scientific). The *CARNS* gene was subcloned into the pcDNA3.2/nFLAG-DEST expression plasmid by the LR reaction (Thermo Fischer Scientific). The SH-SY5Y cells were cultured at 37 °C in DMEM (Wako Pure Chemical Industries, Osaka, Japan) supplemented with 10% FBS. The cells were transfected with *CARNS*/pcDNA3.2/nFLAG-DEST using polyethylenimine Max (Polysciences, Inc., PA, USA). Thereafter, the cells were cultured in the medium containing 400 µg/ml G418. Four weeks after transfection, the surviving clones were isolated and grown on a large scale. The expression of the FLAG-tagged *CARNS* was analyzed by Western blotting using the anti FLAG antibody (Sigma-Aldrich, MO, USA). Stable cell lines with the overexpression of *CARNS* were selected and maintained in the medium containing 400 µg/ml G418.

### ***Cell treatment***

The SH-SY5Y cells stably expressing *CARNS* and the control cells were plated at a density of  $2.0 \times 10^4$  cells/well in 96 well plates

for the MTT assay and at  $4.0 \times 10^6$  cells/dish in a 100-mm dish for the LC-ESI-MS/MS analysis. To investigate the antioxidant capacity of carnosine, the cells were treated with different concentration of  $H_2O_2$  or rotenone for 24 h. The cell viability was determined by using the MTT method (30).

To analyze the formation of 2-oxo-carnosine, the cells were treated with 150  $\mu M$   $H_2O_2$  or 2.5  $\mu M$  rotenone for the various time periods. To examine the effects of ROS on the formation of 2-oxo-carnosine, the cells were pretreated with or without 200 U/mL PEG-catalase for 1 h. After washing with PBS 5 times, the cells were then treated with 150  $\mu M$   $H_2O_2$  or 2.5  $\mu M$  rotenone for 2 h. The cells were washed twice with PBS and collected by using a cell scraper in 1 mL of 80% acetonitrile in water containing stable isotope-labeled standards. After centrifuged at 18,800 g at 4 °C for 20 min, the supernatants were collected, dried, dissolved in 100 mM HCl, and applied on an Oasis MCX cartridge (Waters). The samples were eluted and subjected to LC-ESI-MS/MS by the above-mentioned method.

### **TBARS**

The amount of the TBARS was determined according to the method described by Masaki et al (31). The brains (approximately 10 mg) were homogenized in 0.4 ml of PBS containing 1% Triton X-100. After centrifuged at 18,800 g at 4 °C for 20 min, 50  $\mu l$  of the supernatants were mixed with 0.35 mL of PBS containing 1% Triton X-100 and 0.8 ml of 0.375% 2-thiobarbituric acid, 15% trichloroacetic acid, 2% ethanol, 250 mM HCl, and 0.4% butylhydroxytoluene, then boiled for 15 min. After cooling, the samples were centrifuged (18,800 g, 5 min), and the fluorescence intensities were analyzed by a fluorescence detector (excitation at 515 nm and

emission at 553 nm). Malondialdehyde bis(dimethylacetal) was used as the standard.

### **Measurement of antioxidant activity**

The scavenging effect of 2-oxo-carnosine on a DPPH radical was monitored as previously described (32). Briefly, the reaction mixtures, containing a micromolar range of carnosine, 2-oxo-carnosine, glutathione, or ascorbate, were incubated with 100  $\mu M$  DPPH (Alfa Aesar, MA) in 12 mM sodium phosphate buffer (pH 7.4), containing 40% ethanol, for 30 min at room temperature. The absorbance at 540 nm was measured by a Model 680 plate reader (Bio-Rad, CA, USA). Trolox (MERCK, Darmstadt, Germany) was used as the standard. The radical scavenging activities were evaluated by  $\mu mol$  of Trolox equivalent per mmol of the sample. TEAC was calculated by the equation according to the scavenging percentage of the sample solution to the DPPH radical solution. Consumption of 2-oxo-carnosine and the formation of products were monitored by LC-ESI-MS/MS.

### **Cytotoxicity**

SH-SY5Y cells were plated at a density of  $1.0 \times 10^4$  cells/well in 96 well plates for the MTT assay. To demonstrate the cytoprotective effect of 2-oxo-carnosine against oxidative stress, cells were pretreated with 50  $\mu M$  carnosine or 2-oxo-carnosine for 3 h, then the cells were treated with 2  $\mu M$  rotenone for 24 h. The cell viability was determined using the MTT method.

### **Statistical analysis**

All experiments were performed at least three times. The values for the individual experiments are presented as the means  $\pm$  SD. Statistical significance was determined by the one-way ANOVA, two-way ANOVA or Student's paired t test using GraphPad Prism software.  $P < 0.05$  was considered significant.

**Conflict of interest:** The authors declare that they have no conflicts of interest with the contents of this article.

**Author contributions:** HI and YK contributed equally to this work. HI, YK, and KU designed the study; HI, YK, AY, KK, and TS performed the research; HI, YK, KK, TS, MN, KY and KU analyzed the data; and HI, YK, TS and KU wrote the paper.

## References

1. Boldyrev, A. A., Aldini, G., and Derave, W. (2013) Physiology and Pathophysiology of Carnosine. *Physiol. Rev.* **93**, 1803-1845
2. Drozak, J., Veiga-da-Cunha, M., Vertommen, D., Stroobant, V., and Van Schaftingen, E. (2010) Molecular Identification of Carnosine Synthase as ATP-grasp Domain-containing Protein 1 (ATPGD1). *J. Biol. Chem.* **285**, 9346-9356
3. Drozak, J., Piecuch, M., Poleszak, O., Kozlowski, P., Chrobok, L., Baelde, H. J., and de Heer, E. (2015) UPF0586 Protein C9orf41 Homolog Is Anserine-producing Methyltransferase. *J. Biol. Chem.* **290**, 17190-17205
4. Lenney, J. F. (1990) Separation and characterization of two carnosine-splitting cytosolic dipeptidases from hog kidney (carnosinase and non-specific dipeptidase). *Biol. Chem. Hoppe Seyler* **371**, 433-440
5. Teufel, M., Saudek, V., Ledig, J.-P., Bernhardt, A., Boularand, S., Carreau, A., Cairns, N. J., Carter, C., Cowley, D. J., Duverger, D., Ganzhorn, A. J., Guenet, C., Heintzelmann, B., Laucher, V., Sauvage, C., and Smirnova, T. (2003) Sequence Identification and Characterization of Human Carnosinase and a Closely Related Non-specific Dipeptidase. *J. Biol. Chem.* **278**, 6521-6531
6. Davey, C. L. (1960) The significance of carnosine and anserine in striated skeletal muscle. *Arch. Biochem. Biophys.* **89**, 303-308
7. González-Estrada, M. T., and Freeman, W. J. (1980) Effects of carnosine on olfactory bulb EEG, evoked potentials and DC potentials. *Brain Res.* **202**, 373-386
8. Ikeda, T., Kimura, K., Hama, T., and Tamaki, N. (1980) Activation of Rabbit Muscle Fructose 1, 6-Bisphosphatase by Histidine and Carnosine. *The Journal of Biochemistry* **87**, 179-185
9. Stadtman, E. R. (1992) Protein oxidation and aging. *Science* **257**, 1220-1224
10. Stadtman, E. R., and Levine, R. L. (2003) Free radical-mediated oxidation of free amino acids and amino acid residues in proteins. *Amino Acids* **25**, 207-218
11. Uchida, K. (2003) Histidine and lysine as targets of oxidative modification. *Amino Acids* **25**, 249-257
12. Uchida, K., and Kawakishi, S. (1986) Selective oxidation of imidazole ring in histidine residues by the ascorbic acid — copper ion system. *Biochem. Biophys. Res. Commun.* **138**, 659-665
13. Berg, R. M., Moller, K., and Bailey, D. M. (2011) Neuro-oxidative-nitrosative stress in sepsis. *J. Cereb. Blood Flow Metab.* **31**, 1532-1544
14. Uchida, K., and Kawakishi, S. (1990) Highly site-specific oxygenation of 1-methylhistidine and its analogue with a copper(II)/ascorbate-dependent redox system. *Biochimica et Biophysica Acta (BBA) - General Subjects* **1034**, 347-350
15. Tabakman, R., Jiang, H., Levine, R. A., Kohen, R., and Lazarovici, P. (2004) Apoptotic characteristics of cell death and the neuroprotective effect of homocarnosine on pheochromocytoma PC12 cells exposed to ischemia. *J. Neurosci. Res.* **75**, 499-507

16. Tabakman, R., Lazarovici, P., and Kohen, R. (2002) Neuroprotective effects of carnosine and homocarnosine on pheochromocytoma PC12 cells exposed to ischemia. *J. Neurosci. Res.* **68**, 463-469
17. Uchida, K., and Kawakishi, S. (1989) Ascorbate-mediated specific oxidation of the imidazole ring in a histidine derivative. *Bioorg. Chem.* **17**, 330-343
18. Uchida, K., and Kawakishi, S. (1993) 2-Oxo-histidine as a novel biological marker for oxidatively modified proteins. *FEBS Lett.* **332**, 208-210
19. Kurahashi, T., Miyazaki, A., Suwan, S., and Isobe, M. (2001) Extensive Investigations on Oxidized Amino Acid Residues in H<sub>2</sub>O<sub>2</sub>-Treated Cu,Zn-SOD Protein with LC-ESI-Q-TOF-MS, MS/MS for the Determination of the Copper-Binding Site. *J. Am. Chem. Soc.* **123**, 9268-9278
20. Uchida, K., and Kawakishi, S. (1994) Identification of oxidized histidine generated at the active site of Cu,Zn-superoxide dismutase exposed to H<sub>2</sub>O<sub>2</sub>. Selective generation of 2-oxo-histidine at the histidine 118. *J. Biol. Chem.* **269**, 2405-2410
21. Li, S., Nguyen, T. H., Schoneich, C., and Borchardt, R. T. (1995) Aggregation and precipitation of human relaxin induced by metal-catalyzed oxidation. *Biochemistry* **34**, 5762-5772
22. Meister Winter, G. E., and Butler, A. (1996) Inactivation of Vanadium Bromoperoxidase: Formation of 2-Oxohistidine. *Biochemistry* **35**, 11805-11811
23. Zhao, F., Ghezzi-Schöneich, E., Aced, G. I., Hong, J., Milby, T., and Schöneich, C. (1997) Metal-catalyzed Oxidation of Histidine in Human Growth Hormone: MECHANISM, ISOTOPE EFFECTS, AND INHIBITION BY A MILD DENATURING ALCOHOL. *J. Biol. Chem.* **272**, 9019-9029
24. Retsky, K. L., Chen, K., Zeind, J., and Frei, B. (1999) Inhibition of copper-induced LDL oxidation by vitamin C is associated with decreased copper-binding to LDL and 2-oxo-histidine formation. *Free Radic. Biol. Med.* **26**, 90-98
25. Requena, J. R., Groth, D., Legname, G., Stadtman, E. R., Prusiner, S. B., and Levine, R. L. (2001) Copper-catalyzed oxidation of the recombinant SHa(29–231) prion protein. *Proc. Natl. Acad. Sci. U. S. A.* **98**, 7170-7175
26. Traore, D. A., El Ghazouani, A., Jacquamet, L., Borel, F., Ferrer, J. L., Lascoux, D., Ravanat, J. L., Jaquinod, M., Blondin, G., Caux-Thang, C., Duarte, V., and Latour, J. M. (2009) Structural and functional characterization of 2-oxo-histidine in oxidized PerR protein. *Nat. Chem. Biol.* **5**, 53-59
27. Lee, J. W., and Helmann, J. D. (2006) The PerR transcription factor senses H<sub>2</sub>O<sub>2</sub> by metal-catalysed histidine oxidation. *Nature* **440**, 363-367
28. Stewart, L. C., and Klinman, J. P. (1987) Characterization of alternate reductant binding and electron transfer in the dopamine beta-monooxygenase reaction. *Biochemistry* **26**, 5302-5309
29. Matoba, T., Shimokawa, H., Morikawa, K., Kubota, H., Kunihiro, I., Urakami-Harasawa, L., Mukai, Y., Hirakawa, Y., Akaike, T., and Takeshita, A. (2003) Electron Spin Resonance

- Detection of Hydrogen Peroxide as an Endothelium-Derived Hyperpolarizing Factor in Porcine Coronary Microvessels. *Arterioscler. Thromb. Vasc. Biol.* **23**, 1224-1230
30. Ihara, H., Yamamoto, H., Ida, T., Tsutsuki, H., Sakamoto, T., Fujita, T., Okada, T., and Kozaki, S. (2012) Inhibition of nitric oxide production and inducible nitric oxide synthase expression by a polymethoxyflavone from young fruits of Citrus unshiu in rat primary astrocytes. *Biosci. Biotechnol. Biochem.* **76**, 1843-1848
31. Masaki, N., Kyle, M. E., and Farber, J. L. (1989) tert-butyl hydroperoxide kills cultured hepatocytes by peroxidizing membrane lipids. *Arch. Biochem. Biophys.* **269**, 390-399
32. Yoshida, T., Mori, K., Hatano, T., Okumura, T., Uehara, I., Komagoe, K., Fujita, Y., and Okuda, T. (1989) Studies on inhibition mechanism of autoxidation by tannins and flavonoids. V. Radical-scavenging effects of tannins and related polyphenols on 1,1-diphenyl-2-picrylhydrazyl radical. *Chem. Pharm. Bull. (Tokyo)* **37**, 1919-1921

## FOOTNOTES

This work was supported in part by a Grant-in-Aid for Scientific Research (S) (No. 17H06170) (K.U.), Scientific Research (B) (No. 16H04674) (H.I.), Challenging Exploratory Research (No. 16K13089) (H.I.) and Grant-in-Aid for Scientific Research on Innovative Areas "Oxygen Biology: a new criterion for integrated understanding of life" (No. 26111011) (K.U., H.I., M.N.) of the Ministry of Education, Sciences, Sports, Technology (MEXT), Japan. This research was also supported by AMED-CREST from AMED (K.Y, K.U.), and the Smoking Research Foundation (H.I.)

The abbreviations used are: IDP, imidazole-containing dipeptide; CARNS, carnosine synthase; H<sub>2</sub>O<sub>2</sub>, hydrogen peroxide; HPLC, high performance liquid chromatography; ESI, electrospray ionization; MS, mass spectrometry; MS/MS, tandem MS; TsOH, *p*-toluenesulfonic acid; ANOVA, analysis of variance; MRM, multiple reaction monitor; LOQ, limit of quantitation; SAE, sepsis-associated encephalopathy; LPS, lipopolysaccharide; TBARS, 2-thiobarbituric acid reactive substances; amino-TEMPO•, 4-amino-2,2,6,6-tetramethylpiperidiny1-1-oxy; DMEM, Dulbecco's modified Eagle's medium; MTT, 3-(4,5-dimethylthiazol-2-yl)-2,5-diphenyltetrazolium bromide; TEAC, Trolox equivalent antioxidant capacity; DPPH, 1,1-diphenyl-2-picrylhydrazyl

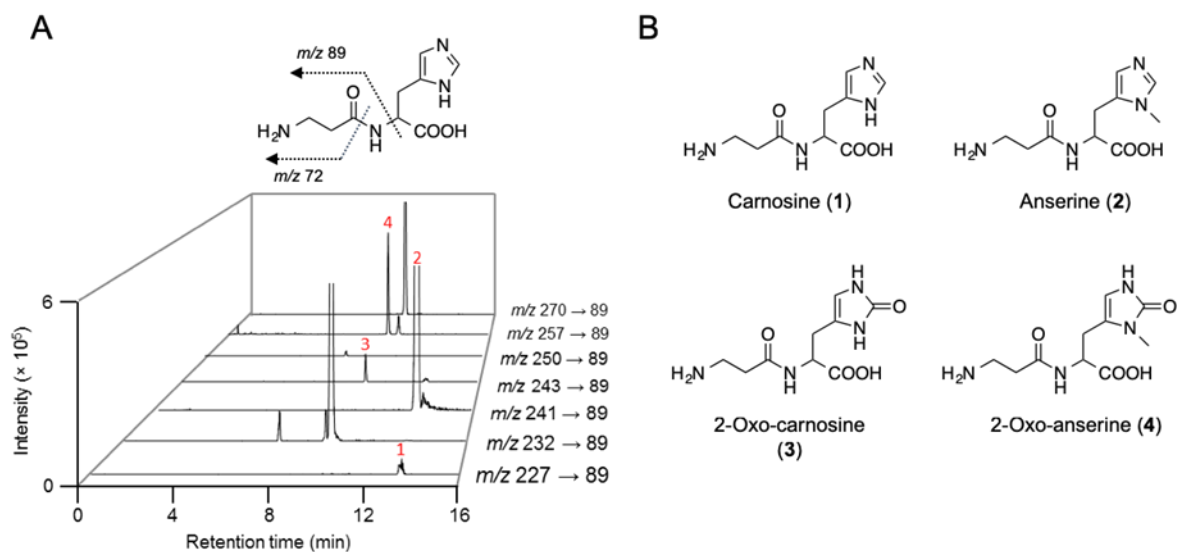


**Figure 1. Simultaneous detection of IDPs in the mouse tissues.** (A) Authentic standards were used for the development of a LC-MS/MS method in the separation and quantification of carnosine and anserine using MS/MS fragments and retention times unique to each IDP (**Fig. S3**). Carnosine, anserine, 2-oxo-carnosine, and 2-oxo-anserine are indicated by 1, 2, 3, and 4, respectively. (B) Chemical structure of carnosine, anserine, 2-oxo-carnosine, and 2-oxo-anserine.

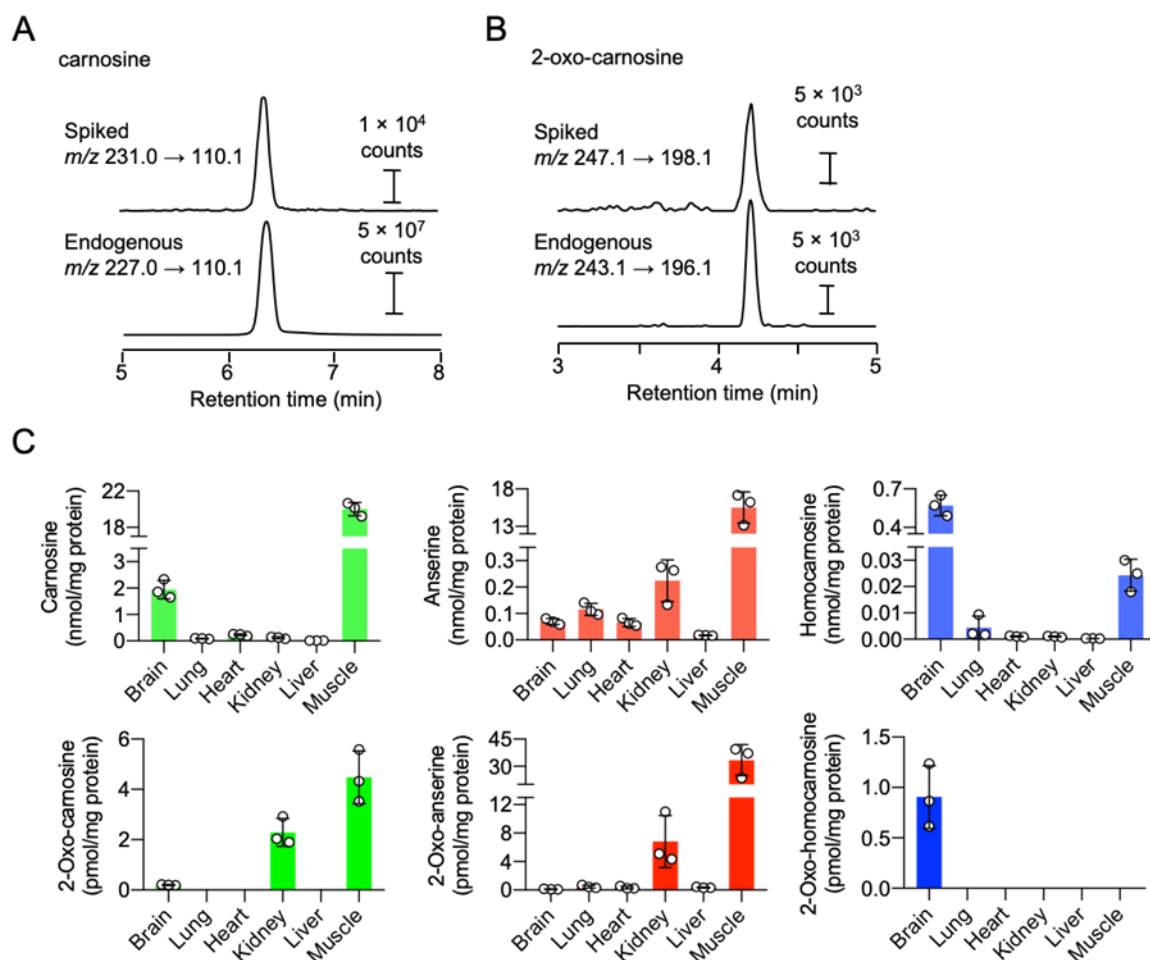


**Figure 2. Quantitative identification of IDPs and oxidized IDPs in mouse tissues.** (A) LC-ESI-MS/MS analysis of endogenous carnosine in the mouse skeletal muscle. Representative LC-ESI-MS/MS chromatograms of spiked isotope-labeled carnosine (upper), and endogenous carnosine (lower) are shown. (B) LC-ESI-MS/MS analysis of endogenous 2-oxo-carnosine in the mouse skeletal muscle. Representative LC-ESI-MS/MS chromatograms of spiked isotope-labeled 2-oxo-carnosine (upper), and endogenous 2-oxo-carnosine (lower) are shown. (C) Quantitative identification of IDPs (upper) and oxidized IDPs (lower) in the mouse tissues. The IDPs and oxidized IDPs in mouse tissues were quantified using LC-ESI-MS/MS coupled with a stable isotope dilution method. Data are mean  $\pm$  SD ( $n = 3$ ).

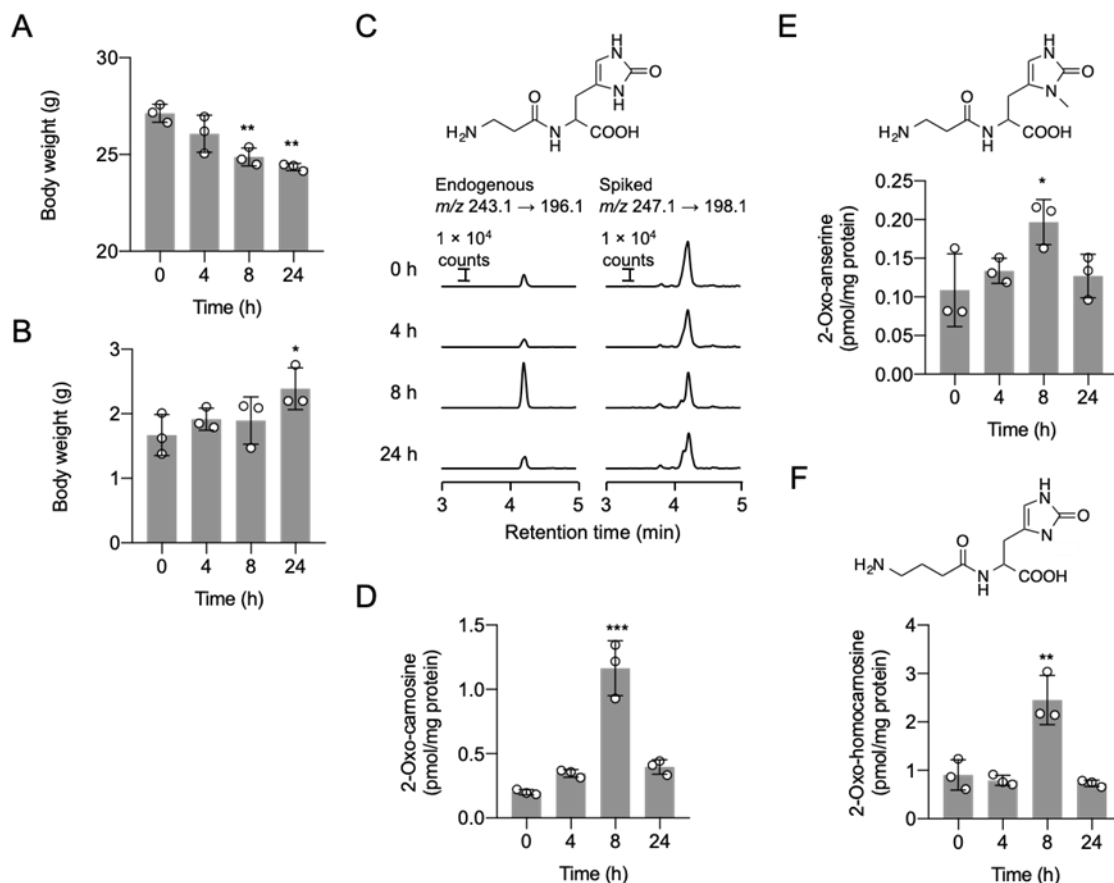


**Figure 3. Generation of oxidized IDPs in brain of SAE model mouse.** Mice were intraperitoneally injected with LPS. (A) Body weights. Graph indicates the body weights of SAE model mice. Data represent means  $\pm$  SD ( $n = 3$ ). One-way ANOVA with the Tukey post hoc test was used for the statistical analysis.  $**P < 0.01$  compared with values for 0 h sample. (B) TBARS levels in brains. Graph indicates the TBARS levels in the brains of an SAE model mice. Data represent means  $\pm$  SD ( $n = 3$ ). One-way ANOVA with the Tukey post hoc test was used for the statistical analysis.  $*P < 0.05$  compared with values for 0 h sample. (C) LC-ESI-MS/MS analysis of endogenous 2-oxo-carnosine in brain of an SAE model mouse. Representative LC-ESI-MS/MS chromatograms of endogenous- (left) and spiked isotope-labeled 2-oxo-carnosine (right) are shown. (D) Bar graph which indicates the levels of 2-oxo-carnosine. Data represent means  $\pm$ SD ( $n = 3$ ). One-way ANOVA with the Tukey post hoc test was used for the statistical analysis.  $***P < 0.001$  compared with values for 0 h sample. (E) Quantitative identification of 2-oxo-anserine in brain of an SAE model mouse. 2-Oxo-anserine was quantified using LC-ESI-MS/MS coupled with a stable isotope dilution method. Data represent means  $\pm$ SD ( $n = 3$ ). One-way ANOVA with the Tukey post hoc test was used for the statistical analysis.  $*P < 0.05$  compared with values for 0 h sample. (F) Quantitative identification of 2-oxo-homocarnosine in brain of an SAE model mouse. 2-Oxo-homocarnosine was quantified using LC-ESI-MS/MS coupled with a stable isotope dilution method. Data represent means  $\pm$ SD ( $n = 3$ ). One-way ANOVA with the Tukey post hoc test was used for the statistical analysis.  $**P < 0.01$  compared with values for 0 h sample.

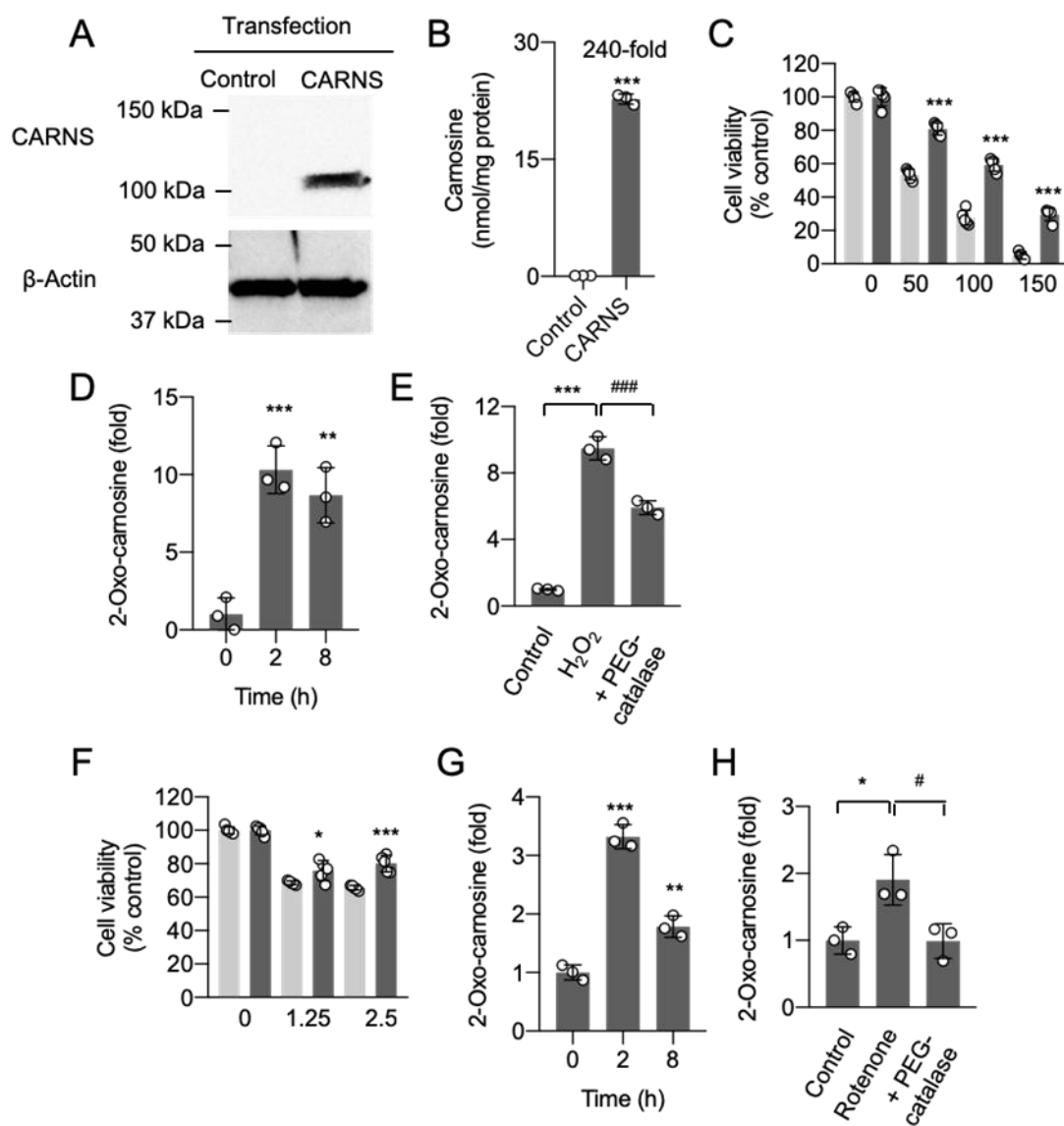


**Figure 4. Formation of 2-oxo-carnosine in the SH-SY5Y cells stably expressing CARNS under oxidative stress.** (A) Western blotting showing CARNS protein levels in the SH-SY5Y cells stably expressing CARNS and in the control cells. Expression of FLAG-tagged CARNS in the SH-SY5Y cells was analyzed using the anti-FLAG antibody.  $\beta$ -Actin was used as a loading control. (B) Quantitative identification of carnosine in the SH-SY5Y cells stably expressing CARNS and in the control cells. Carnosine was quantified using LC-ESI-MS/MS coupled with a stable isotope dilution method. Data represent means  $\pm$ SD ( $n = 3$ ). Student's paired t-test was used for the statistical analysis. \*\*\* $P < 0.001$  compared with values for the control. (C) Cytotoxicity induced by  $H_2O_2$  in the SH-SY5Y cells stably expressing CARNS (black) and in the control cells (gray). Cell viability was determined by the MTT assay. Data represent means  $\pm$ SD ( $n = 5$ ). Two-way ANOVA with the Bonferroni post hoc test was used for the statistical analysis. \*\*\* $P < 0.001$  compared with values for control. (D) Quantitative identification of endogenous 2-oxo-carnosine in the SH-SY5Y cells stably expressing CARNS treated with  $H_2O_2$ . 2-Oxo-carnosine was quantified using LC-ESI-MS/MS

coupled with a stable isotope dilution method. Data represent means  $\pm$ SD ( $n = 5$ ). Two-way ANOVA with the Bonferroni post hoc test was used for the statistical analysis.  $**P < 0.01$  and  $***P < 0.001$  compared with values for control. (E) Inhibition of 2-oxo-carnosine formation by PEG-catalase. The CARNS expressing cells were pretreated with PEG-catalase. After washing, the  $H_2O_2$ -induced cytotoxicity was assessed. Data represent means  $\pm$ SD ( $n = 3$ ). One-way ANOVA with the Tukey post hoc test was used for the statistical analysis.  $***P < 0.001$  compared with values for 0 h sample.  $###P < 0.001$  compared with values for  $H_2O_2$  treatment. (F) Cytotoxicity induced by rotenone in the SH-SY5Y cells stably expressing CARNS (black) and in the control cells (gray). Cell viability was determined by the MTT assay. Data represent means  $\pm$ SD ( $n = 5$ ). Two-way ANOVA with the Bonferroni post hoc test was used for statistical analysis.  $*P < 0.05$  and  $***P < 0.001$  compared with values for control. (G) Quantitative identification of endogenous 2-oxo-carnosine in the SH-SY5Y cells stably expressing CARNS treated with rotenone. 2-Oxo-carnosine was quantified using LC-ESI-MS/MS coupled with a stable isotope dilution method. Data represent means  $\pm$ SD ( $n = 3$ ). One-way ANOVA with the Tukey post hoc test was used for the statistical analysis.  $**P < 0.01$  and  $***P < 0.001$  compared with values for the control. (H) Inhibition of 2-oxo-carnosine formation by PEG-catalase. The CARNS expressing cells were pretreated with PEG-catalase. After washing, the rotenone-induced cytotoxicity was assessed. Data represent means  $\pm$ SD ( $n = 3$ ). One-way ANOVA with the Tukey post hoc test was used for the statistical analysis.  $***P < 0.001$  compared with values for control.  $###P < 0.001$  compared with values for the rotenone treatment.

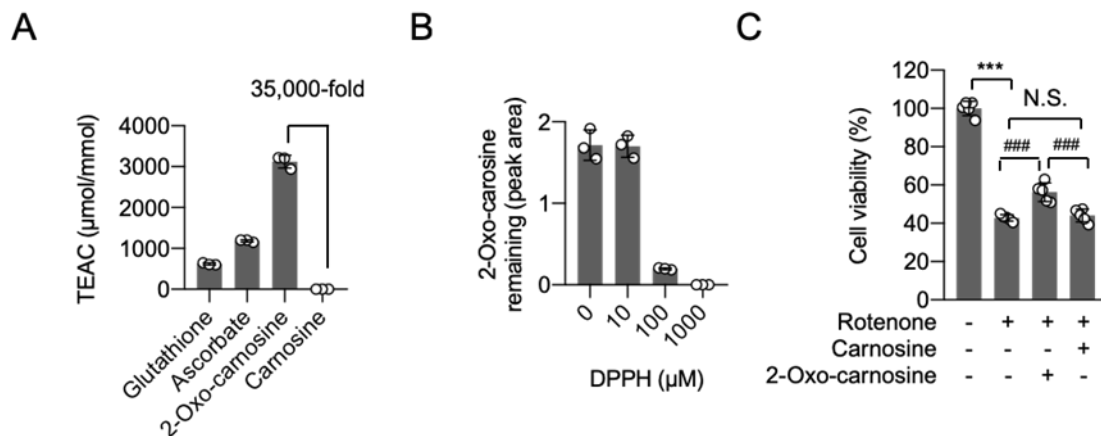


**Figure 5. Gain of antioxidant function.** (A) Comparison of DPPH radical scavenging activity of 2-oxo-carnosine with the antioxidants. The data are expressed as  $\mu\text{mol}$  of Trolox equivalent per  $\text{mmol}$  of samples. (B) Consumption of 2-oxo-carnosine upon incubation with DPPH. (C) Cytoprotective effect of 2-oxo-carnosine against rotenone-induced neuronal cell death. Cell viability was determined by the MTT assay. Data represent means  $\pm$ SD ( $n = 5$ ). One-way ANOVA with the Tukey post hoc test was used for the statistical analysis. \*\*\* $P < 0.001$  compared with values for control. ### $P < 0.001$  compared with values for rotenone treatment. N.S., not significant.

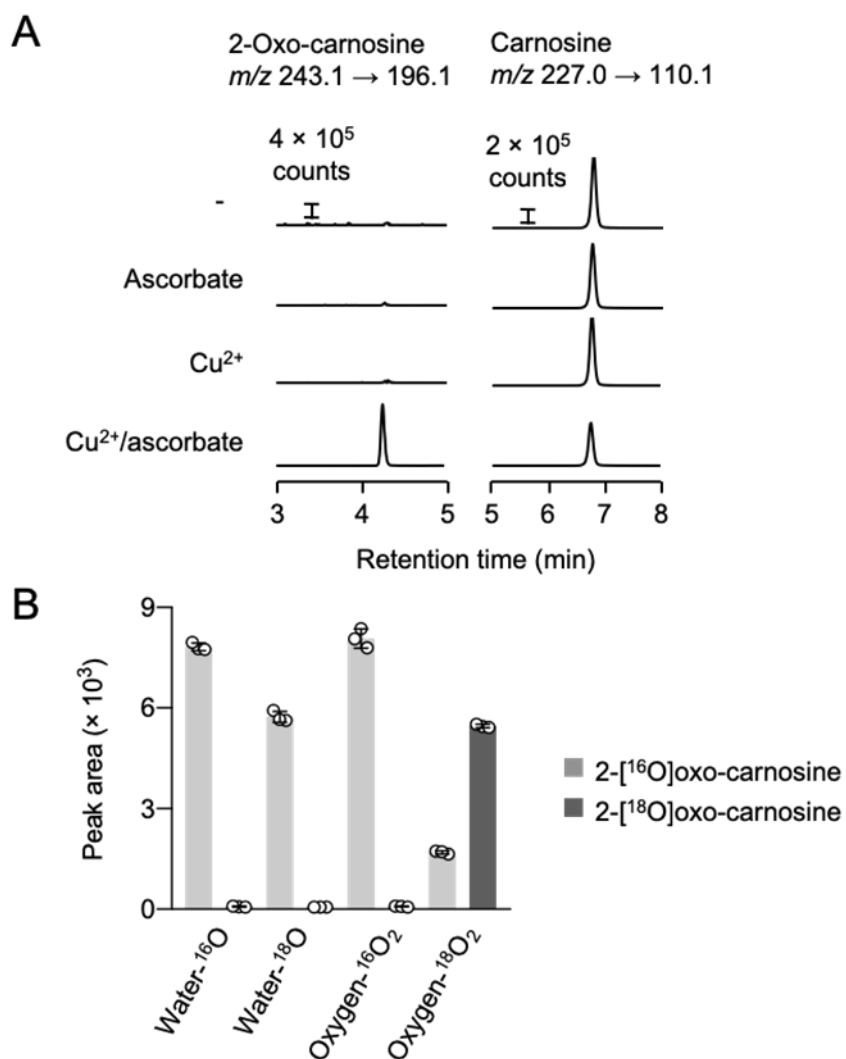


**Figure 6. Mechanism for the conversion of carnosine to 2-oxo-carnosine.** (A) LC-ESI-MS/MS analysis of formation of 2-oxo-carnosine by metal-catalyzed oxidation. Ten mM Carnosine was incubated in 200 mM sodium phosphate buffer (pH 7.2) in the presence or absence of 200 mM ascorbate or 2 mM CuSO<sub>4</sub> at room temperature with the bubbling of oxygen gas for 30 min. Representative LC-ESI-MS/MS chromatograms of carnosine (right) and 2-oxo-carnosine (left) are shown. (B) Incorporation of oxygen at C2 position of 2-oxo-carnosine. The degassed reaction mixture containing 0.5 mM carnosine, 100 mM sodium phosphate buffer (pH 7.2), and 50 mM ascorbate was prepared using water-<sup>16</sup>O or water-<sup>18</sup>O. Oxygen-<sup>16</sup>O<sub>2</sub> or -<sup>18</sup>O<sub>2</sub> gas was bubbled into the mixture. Metal-catalyzed oxidation was started by the addition of 1/100 volume of 50 mM CuSO<sub>4</sub>, and then the mixtures were incubated for 5 min at room temperature. The samples were analyzed by LC-ESI-MS/MS.

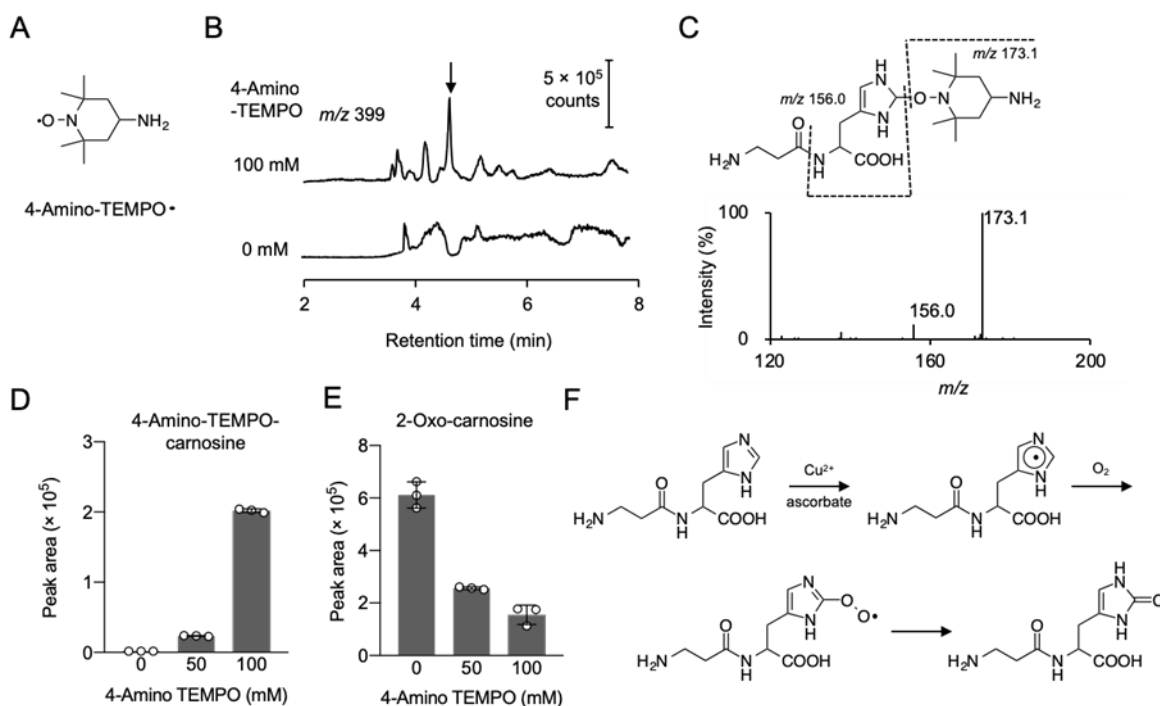


**Figure 7. Analysis of radical intermediate of carnosine by amino-TEMPO.** (A) Chemical structure of 4-amino-TEMPO•. (B) Mass chromatograph of putative carnosine-amino TEMPO adduct. The reaction mixtures containing 5 mM carnosine, 500 mM sodium phosphate buffer (pH 7.2), 50 mM ascorbate, 0.5 mM  $\text{CuSO}_4$ , and 4-amino-TEMPO (0 or 100 mM) were incubated with bubbling oxygen gas at room temperature for 30 min. The samples were subjected to HPLC-ESI-MS monitoring at  $m/z$  399. (C) Collision-induced dissociation of the  $[M + H]^+$  of putative carnosine-amino TEMPO adduct at  $m/z$  399 at a collision energy of 10 V. (D) Formation of carnosine-amino TEMPO adduct. The reaction mixtures containing 5 mM carnosine, 500 mM sodium phosphate buffer (pH 7.2), 50 mM ascorbate, 0.5 mM  $\text{CuSO}_4$ , and 4-amino-TEMPO (0, 50, or 100 mM) were incubated with bubbling oxygen gas at room temperature for 30 min. The samples were analyzed by LC-ESI-MS/MS with MRM ( $m/z$  399 $\rightarrow$ 173). (E) Inhibition of 2-oxo-carnosine formation by 4-amino-TEMPO. The same samples were analyzed by LC-ESI-MS/MS with MRM ( $m/z$  243 $\rightarrow$ 196). (F) Proposed mechanism of the mono-oxygenation of the IDPs.

**2-Oxo-histidine-containing dipeptides are functional oxidation products**  
Hideshi Ihara, Yuki Kakihana, Akane Yamakage, Kenji Kai, Takahiro Shibata,  
Motohiro Nishida, Ken-ichi Yamada and Koji Uchida

*J. Biol. Chem.* published online November 30, 2018

---

Access the most updated version of this article at doi: [10.1074/jbc.RA118.006111](https://doi.org/10.1074/jbc.RA118.006111)

Alerts:

- [When this article is cited](#)
- [When a correction for this article is posted](#)

[Click here](#) to choose from all of JBC's e-mail alerts

*Supporting Information*

**2-Oxo-histidine-containing dipeptides are functional oxidation products**

Hideshi Ihara<sup>†</sup>, Yuki Kakihana<sup>†</sup>, Akane Yamakage<sup>†</sup>, Kenji Kai<sup>#</sup>, Takahiro Shibata<sup>¶</sup>, Motohiro Nishida<sup>††</sup>, Ken-ichi Yamada<sup>‡, ||</sup>, and Koji Uchida<sup>§, ¶, ||</sup>

**Address:**

<sup>†</sup>Department of Biological Science, Graduate School of Science, Osaka Prefecture University, Sakai, Osaka 599-8531, Japan

<sup>#</sup>Department of Biological Chemistry, Graduate School of Life and Environmental Sciences, Osaka Prefecture University, Sakai, Osaka 599-8531, Japan

<sup>¶</sup>Graduate School of Bioagricultural Sciences, Nagoya University, Nagoya 464-8601, Japan

<sup>††</sup>Division of Cardiocirculatory Signaling, National Institute for Physiological Sciences, Okazaki 444-8787, Japan

<sup>‡</sup>Physical Chemistry for Life Science Laboratory, Faculty of Pharmaceutical Sciences, Kyushu University, Fukuoka, Japan.

<sup>||</sup>Japan Agency for Medical Research and Development, CREST, Tokyo, Japan.

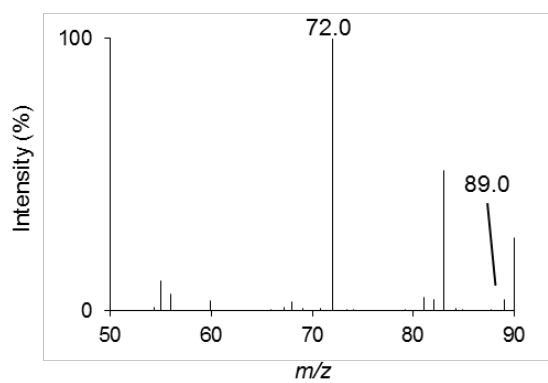
<sup>§</sup>Graduate School of Agricultural and Life Sciences, The University of Tokyo, Tokyo 113-8657, Japan

**Table S1**

Analyte	Precursor ion (m/z)	Product ion (m/z)	Collision energy (V)
Carnosine	227.0	110.1	20
Carnosine*	231.0	110.1	20
Anserine	241.0	109.1	25
Anserine*	245.0	109.1	25
Homocarnosine	241.1	156.0	10
Homocarnosine*	244.1	159.0	10
2-Oxo-carnosine	243.1	196.1	10
2-Oxo-carnosine*	247.1	198.1	10
2-Oxo-anserine	257.2	169.1	15
2-Oxo-anserine*	261.1	169.1	15
2-Oxo-homocarnosine	257.1	172.0	15
2-Oxo-homocarnosine*	260.1	175.0	15

\*Stable isotope-labeled derivatives

A



B

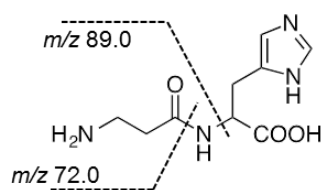


Fig. S1. Collision-induced dissociation of carnosine. (A) mass spectrum of fragment ions dissociated from carnosine at a collision energy of 10 V. (B) chemical structure of carnosine. Cleavage sites were indicated by dashed lines.

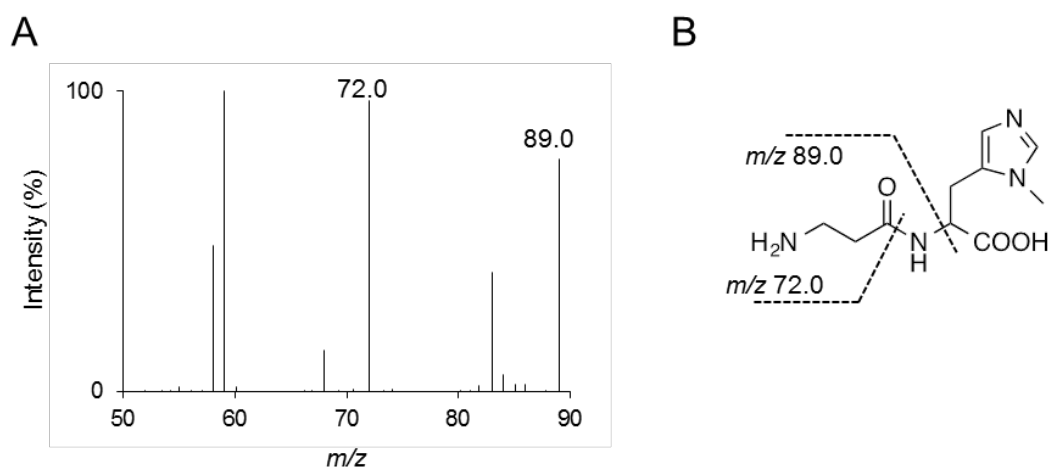


Fig. S2. Collision-induced dissociation of anserine. (A) mass spectrum of fragment ions dissociated from anserine at a collision energy of 10 V. (B) chemical structure of anserine. Cleavage sites were indicated by dashed lines.

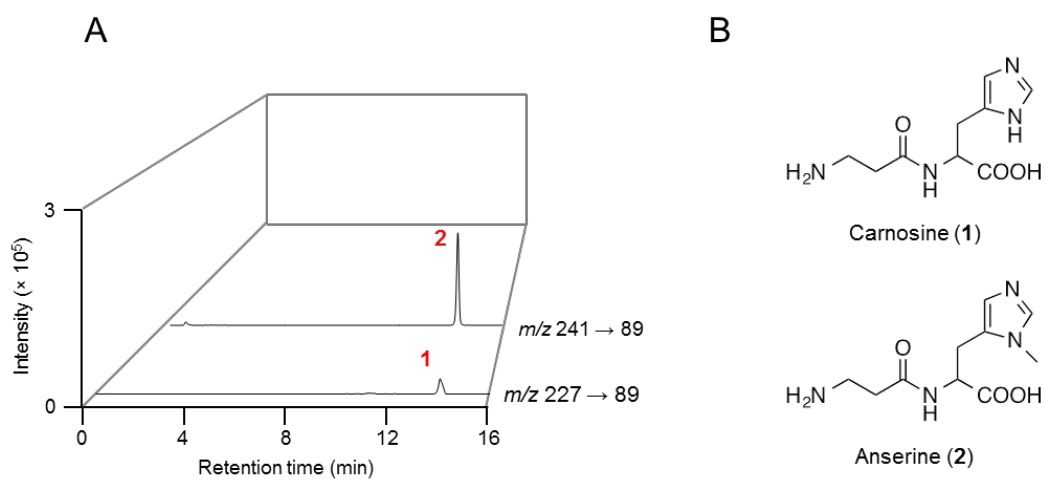


Fig. S3. Adductome analysis of authentic IDPs. (A) adductome maps of authentic carnosine and anserine indicated by 1 and 2, respectively. (B) chemical structure of carnosine and anserine.

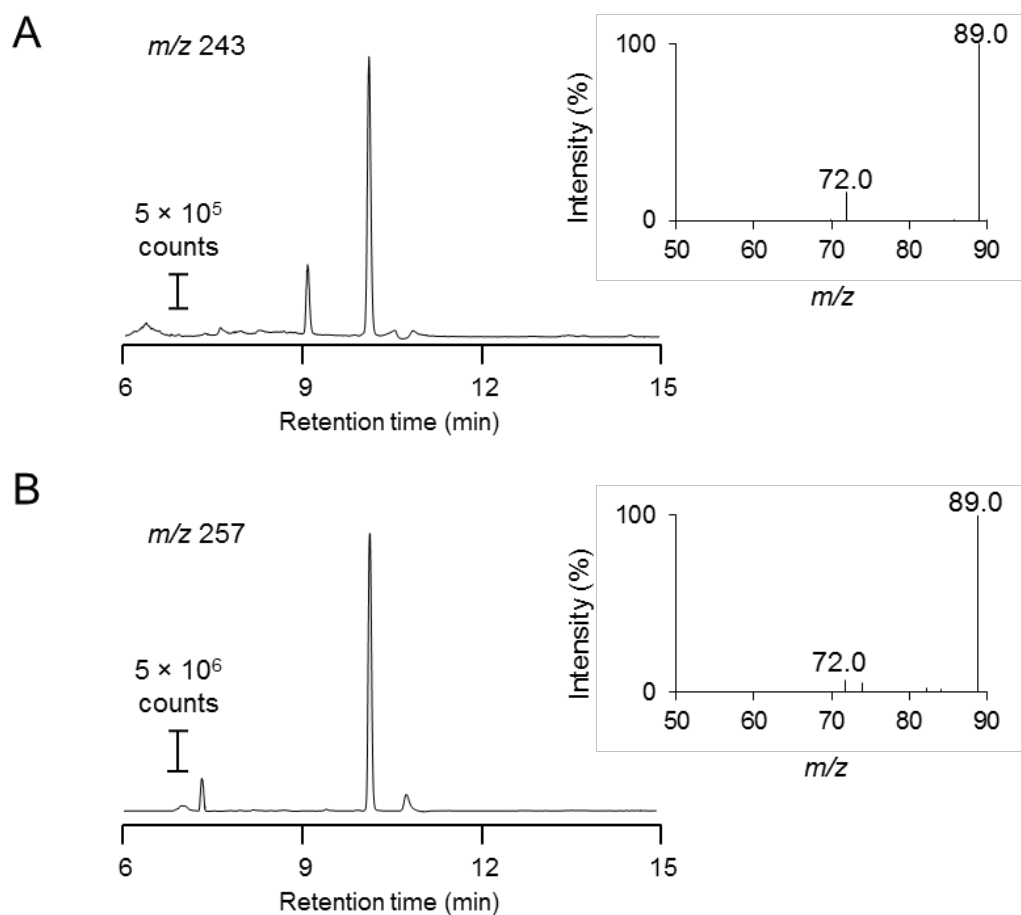


Fig. S4. Identification of authentic oxidized IDPs. (A) mass chromatogram of oxidized carnosine at *m/z* 243 (left) and collision-induced dissociation of oxidized carnosine at a collision energy of 15 V. (B) mass chromatogram of oxidized anserine at *m/z* 257 (left) and collision-induced dissociation of oxidized anserine at a collision energy of 15 V.

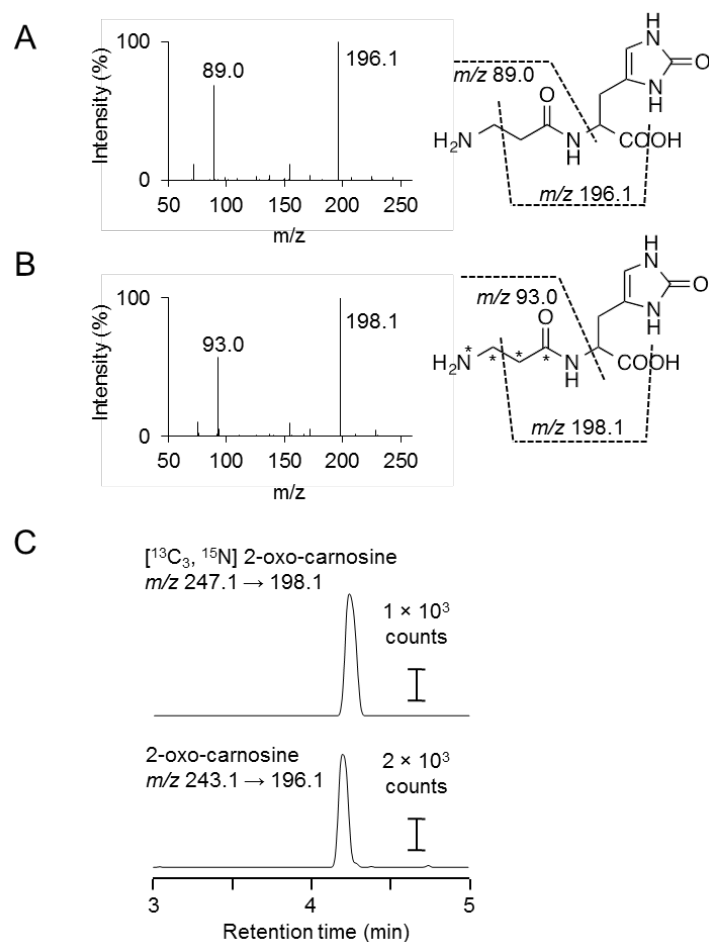


Fig. S5. LC-ESI-MS/MS analysis of purified 2-oxo-carnosine. (A) Collision-induced dissociation of purified 2-oxo-carnosine. Mass spectrum of fragment ions dissociated from 2-oxo-carnosine at a collision energy of 15 V (left) and chemical structure of 2-oxo-carnosine indicating cleavage sites by dashed lines (right). (B) Collision-induced dissociation of purified 2-oxo-carnosine labeled with  $^{13}\text{C}$ . Mass spectrum of fragment ions dissociated from  $^{13}\text{C}$ -labeled 2-oxo-carnosine at a collision energy of 15 V (left) and chemical structure of  $^{13}\text{C}$ -labeled 2-oxo-carnosine indicating cleavage sites by dashed lines (right). Positions of  $^{13}\text{C}$  were indicated by asterisks. (C) Representative LC-ESI-MS/MS chromatograms of the standard  $^{13}\text{C}$ -labeled carnosine (upper) and nonlabeled carnosine (lower) using MRM between the transition from the protonated parent ions  $[\text{M} + \text{H}]^+$  to the characteristic daughter ions,  $m/z$  247.1 $\rightarrow$ 198.1 and  $m/z$  243.1 $\rightarrow$ 196.1.

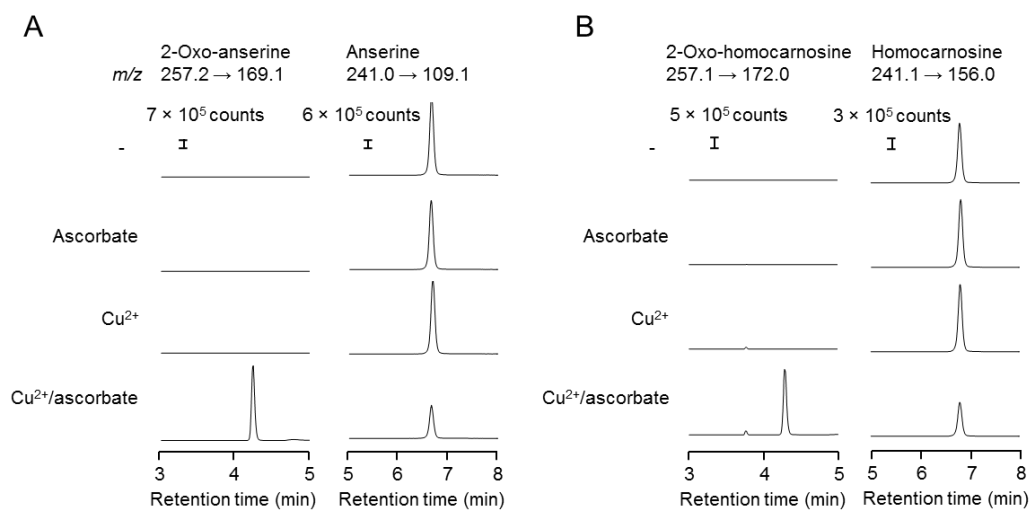


Fig. S6. LC-ESI-MS/MS analysis of formation of 2-oxo-anserine (A) and 2-oxo-homocarnosine (B) by metal-catalyzed oxidation. 10 mM Anserine and homocarnosine were incubated in 200 mM sodium phosphate buffer (pH 7.2) in the presence or absence of 200 mM ascorbate or 2 mM CuSO<sub>4</sub> at room temperature with bubbling of oxygen gas for 30 min. Representative LC-ESI-MS/MS chromatograms of anserine and homocarnosine (right) and oxidized forms (left) are shown.